THE JOURNAL OF PHYSICAL CHEMISTRY B

Article

pubs.acs.org/JPCB

Pressure-Induced Phase Transition in N−H···O Hydrogen-Bonded Molecular Crystal Oxamide

Tingting Yan,[†,§] Shourui Li,[†,§] Kai Wang,[†] Xiao Tan,[†] Zhangmei Jiang,[†] Ke Yang,[‡] Bingbing Liu,[†] Guangtian Zou,[†] and Bo Zou*[,†]

[†]State Key Laboratory of Superhard Materials, Jilin University, Changchun 130012, China

[‡]Shanghai Synchrotron Radiation Facilities, Shanghai Institute of Applied Physics, Chinese Academy of Sciences, Shanghai 201204, China

Supporting Information

ABSTRACT: The effect of high pressure on the structural stability of oxamide has been investigated in a diamond anvil cell by Raman spectroscopy up to ∼14.6 GPa and by angle-dispersive X-ray diffraction (ADXRD) up to ∼17.5 GPa. The discontinuity in Raman shifts around 9.6 GPa indicates a pressure-induced structural phase transition. This phase transition is confirmed by the change of ADXRD spectra with the symmetry transformation from $P\bar{1}$ to $P1$. On total release of pressure, the diffraction pattern returns to its initial state, implying this transition is reversible. We discuss the pressure-induced variations in N−H stretching vibrations and the amide modes in Raman spectra and propose that this phase transition is attributed to the distortions of the hydrogen-bonded networks.

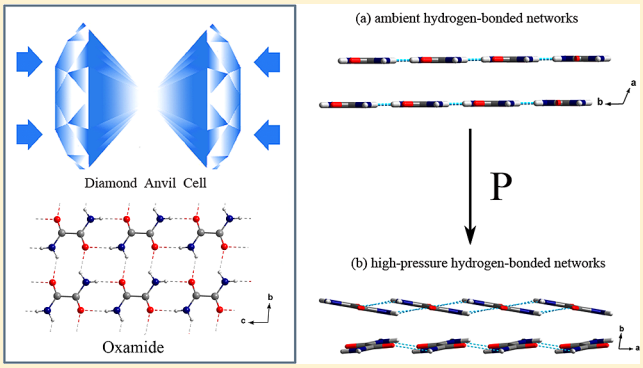

INTRODUCTION

Hydrogen-bonded molecular crystals under high-pressure conditions have always been the subject of extensive research and gotten abundant phenomena.[1−5] Especially, amides are of particular interest because they are widespread in nature and have special applications in industry and technology as structural materials.[6−8] Moreover, the hydrogen bonds in the functional group of amides have the directionality as in carboxylic acid synthon. In 1937, P. W. Bridgman selected oxamide ($(CONH_2)_2$) as a model in his scientific research.[9,10] In his investigations, four polymorphs were observed, but he did not identify them. Subsequently, the molecular and crystal structures of oxamide attracted considerable interest of structural chemists. The form of oxamide that is stable at room temperature is triclinic.[11] In 1977, the accurate and complete data of this structure was confirmed by G. de With and S. Harkema.[12] Another structure of oxamide is the metastable orthorhombic form, which can revert spontaneously to the triclinic form on standing at room temperature.[13] Herein, we conduct research on oxamide with more accurate methods, aiming to get much valuable information for the structural stability of this material under high pressure. Oxamide is one of the simplest amides involving N−H···O hydrogen bonds. Crystallographic studies have established the molecule possesses a center of symmetry chosen to be at (0, $^1/_2$, $^1/_2$).[11] Oxamide is a kind of composite molecule containing peptide linkages, which constitute a representative molecular feature of proteins. There is a formal σ-bond between the two amidic carbon atoms. Therefore, the knowledge of pressure-induced behaviors of amides is of fundamental and significant importance for physics, chemistry, and life science.

Hydrogen bonds are the most pervasive and important directional intermolecular interactions in biological systems, inorganic materials, organic materials, and hybrid compounds.[14−18] In addition, the research on hydrogen bonds using high-pressure techniques in supramolecular chemistry paves the new way for molecular construction in crystal engineering.[19−22] It is well established that pressure can reduce the intermolecular distance of materials and bring the atoms closer to each other.[23,24] This means that pressure has the ability to tune the strength of hydrogen bonds.[25] The increase of pressure can enhance the strength of weak and moderate D−H···A bonds (D and A mean donor and acceptor, respectively), resulting in the elongated D−H distance, whereas it has no such effect on strong hydrogen bonds.[26,27] The pressure-induced changes of hydrogen bonds can also lead to the transition of crystal symmetry, usually combined with the effect of π-stacking, van der Waals, and electrostatic interactions.[28,29] Thus, variations in hydrogen bonds and the cooperativity of various noncovalent interactions as a function of pressure play a crucial role for the structural stability of materials.

Received: March 16, 2012
Revised: July 20, 2012
Published: July 20, 2012

ACS Publications © 2012 American Chemical Society

dx.doi.org/10.1021/jp302575k | J. Phys. Chem. B 2012, 116, 9796−9802

As shown in Figure 1, oxamide exhibits a typical layered structure of organic molecules with two-dimensional (2D)

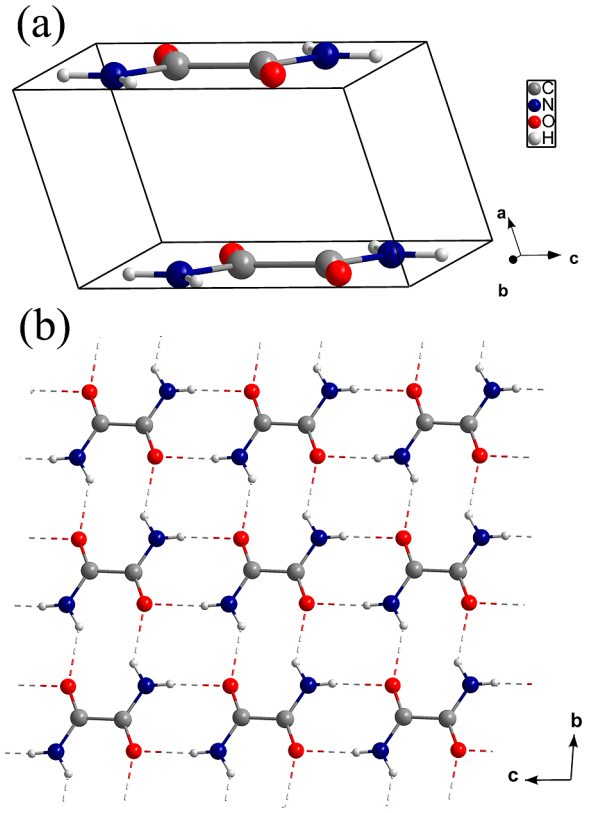

Figure 1. Crystal structure of oxamide under ambient conditions: (a) the unit cell; (b) the typical 2D rosette of hydrogen bonds in the *bc*-plane; the hydrogen bonds are marked as dashed lines.

hydrogen-bonded sheets under ambient conditions. It crystallizes into the triclinic $P\bar{1}$ structure, with the unit cell parameters $a = 3.61(8)$ Å, $b = 5.18(0)$ Å, $c = 5.65(1)$ Å, and $\beta = 113.97(1)°$ in a unit cell. In its structure, there is one molecule in the unit cell and the molecule resides on the *bc*-plane. Within the plane, each molecule is linked to four neighbor molecules by hydrogen bonds, while there is relatively weak van der Waals interaction between these planes only. Each molecule participates in the formation of eight hydrogen bonds with four donors and four acceptors via the bidentate interaction of the N—H and C═O groups. Consequently, the structural stability of oxamide under high pressure is determined predominately by the balance between hydrogen bonds and van der Waals interactions.

In this work, we have performed high-pressure in situ Raman scattering measurements up to ~14.6 GPa and angle-dispersive X-ray diffraction (ADXRD) studies up to ~17.5 GPa on oxamide. The detailed structural information under high pressure can be obtained by analysis of ADXRD pattern at 9.7 GPa. We propose that this transition is due to the distortions of hydrogen bonds, demonstrated by variations in N−H stretching modes in Raman spectra. This research also provides a better understanding of the nature of hydrogen bonds, as well as the structural stability of hydrogen-bonded molecular crystals.

EXPERIMENTAL SECTION

Oxamide was purchased from Sigma-Aldrich Co. and used without further purification. Powder samples for high-pressure measurements were prepared by crushing single crystals in an agate mortar. The diamond anvil cell (DAC) with a culet face of 600 μm in diameter was applied for in situ Raman scattering and angle-dispersive X-ray diffraction (ADXRD) measurements at room temperature. A T301 steel gasket was preindented to 60 μm, and then, a center hole with a diameter of 200 μm was drilled as the sample chamber. Subsequently, oxamide was placed in the gasket hole together with a small ruby chip to determine the pressure using the standard ruby-fluorescence method.[30] A methanol−ethanol−water mixture of 16:3:1 by volume was used as the pressure-transmitting medium (PTM). The ruby lines were found to be sharp and well separated to the highest pressure in our studies.

Raman measurements were conducted with the Renishaw inVia Raman microscope. The 633 nm line of an argon ion laser was employed to excite the sample. The incident and output power of the laser were both set to 10 mW. Prior to each measurement, the spectrometer was calibrated with the standard Si line. The resolution of the system was about 1 cm^{-1}. Furthermore, considering the effect of pressure conditions (hydrostatic pressure, quasi-hydrostatic pressure, and nonhydrostatic pressure), we conduct two other runs of high-pressure Raman scattering investigations; one was carried out with liquid argon as the PTM, and one without any PTM. In the case of the layered structure of oxamide, which makes it a soft material, the absence of PTM will not much affect the high-pressure behavior.[31] The data under different pressure conditions are essentially the same, guaranteeing the accuracy of the experimental results (Figure S1, Supporting Information).

ADXRD experiments were carried out on HPCAT's beamline of the Advanced Photon Source at Argonne National Laboratory. The 0.40546 Å beam was adopted as the incidence light source. Portions of this work were performed on the 4W2 beamline at the High Pressure Station of the Beijing Synchrotron Radiation Facility (BSRF). Portions of this work were performed on the BL15U1 beamline at the Shanghai Synchrotron Radiation Facility (SSRF). CeO_2 was used as the standard sample to do the calibration before data collection. The Bragg diffraction rings were recorded using a Mar345 imaging-plate detector. The two-dimensional XRD images were analyzed using the Fit2D program, yielding one-dimensional intensity versus diffraction angle 2θ patterns.[32] Further analysis was performed by the Rietveld method using the Materials Studio 5.0 Reflex program suite to gain accurate lattice parameters and possible space groups.

RESULTS AND DISCUSSION

The Raman modes of oxamide are assigned on the basis of the reported literature.[33,34] Figure 2 presents the Raman spectra in the frequency range 100−350 cm^{-1} at various pressures. Figure 3 shows the pressure-induced frequency shifts of these modes. As shown in Figure 2, oxamide has three lattice modes marked by the arrows under ambient conditions. The lattice region is decomposed into three modes for clarity (labeled from 1 to 3 from low to high frequencies). With increasing pressure, these modes overlap and cross each other by virtue of different shift rates. Meanwhile, the relative intensities of the three modes change gradually. At 3.2 GPa, mode 2 has the highest intensity

dx.doi.org/10.1021/jp302575k | J. Phys. Chem. B 2012, 116, 9796−9802

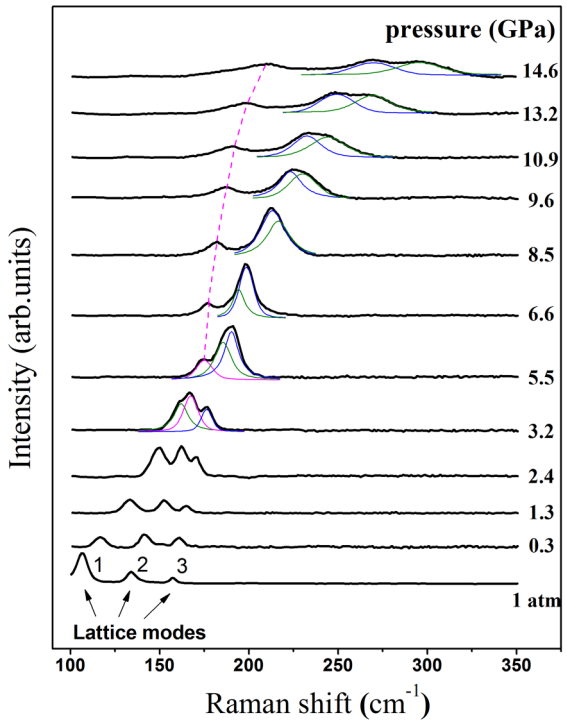

Figure 2. Selected Raman spectra of lattice modes of oxamide at various pressures in the range 100−350 cm^{-1}. The decompositions of the lattice region into three modes are illustrated for clarity. The dotted line presents the specified lattice mode's evolution.

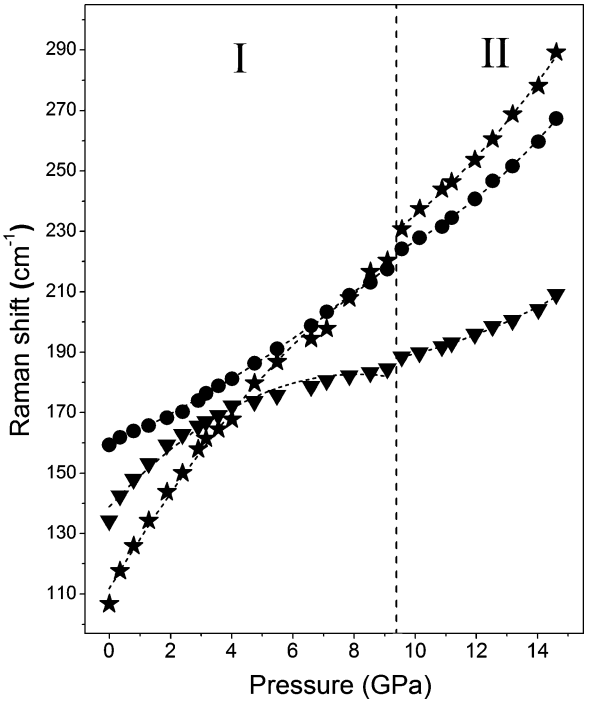

Figure 3. Frequency shifts of the lattice modes. Fitting curves are performed for clarity. The vertical dotted line represents the boundary of the two phases.

among these modes. Above this pressure, the intensity of this mode reduces to be the lowest one while there is a remarkable increase in the intensity of mode 3 up to 8.5 GPa. At pressures higher than 8.5 GPa, mode 3 with respect to mode 1 shows reduction in relative intensity.

As can be seen in Figures 2 and 3, all of the peaks shift gradually toward higher frequencies as a function of pressure, originating from the increased strength of the intermolecular interactions with the reduction of intermolecular distances. In Figure 3, the nonlinear shifts of these modes are fitted to quadratic functions. An obvious discontinuity between the two regions is observed, indicating that oxamide undergoes a phase transition from phase I to phase II at ∼9.6 GPa. As can be seen, pressure dependences of lattice modes are less sensitive in phase II than in phase I. This suggests phase II is more stable than phase I by reason of close packing.

Raman spectra of oxamide ranging from 350 to 2000 cm^{-1} and the pressure dependence of these modes are depicted in Figures 4 and 5, respectively. At 0.3 GPa, a new peak marked by an asterisk emerges at 788 cm^{-1}, which could be identified as the N—H bending (amide II) vibration mode.[35] Furthermore, this mode shifts to lower frequency constantly after 9.6 GPa, demonstrating the proposed phase transition is caused by the distortions of the hydrogen bonds. When the pressure reaches near 5 GPa, due to the softening of the skeletal vibration, the peak of the C—C stretching mode loses its intensity absolutely. At the critical pressure of the transition, the mode assigned to NH_2 rocking displays an abrupt red shift, reduced by about 2 cm^{-1}, which can be interpreted as the local distortion of amino groups. Peak positions of δ(NH) and $\rho(NH_2)$ are shown in Table S1 in the Supporting Information. Meanwhile, the blue shifts of the NH_2 bending mode (amide II) and NH_2 rocking mode up to 9.6 GPa imply the existence of weak or moderate strength hydrogen bonds in oxamide. Above this pressure, the obvious broadening of the NH_2 rocking mode can be explained in terms of the sensibility to the distorted hydrogen bond networks. Furthermore, it is significant to note the behavior of the pressure-induced frequency shifts for the C═O stretching mode (amide I), which is almost constant between 1 atm and 9 GPa. An increase of pressure should decrease the distance between O atoms and C atoms. However, the N—H···O═C hydrogen bonds elongate this distance, counteracting partial pressure effects. The other vibrations, including the C—N stretching mode (amide III), exhibit blue shifts throughout the whole pressure region as we expect owing to the decrease in the bond distances and the enhancement in the interatomic interactions.[36,37] As can be seen, all of these internal modes show changes in slope across the transition pressure.

Figure 6 summarizes the evolution of N−H stretching vibrations. The modes of methanol−ethanol−water mixture are marked by a rhombus. The bands at 3116 and 3151 cm^{-1} are assigned to symmetric N−H stretching vibrations at ambient pressure, while the band at 3384 cm^{-1} corresponds to asymmetric stretching vibration. As can be seen, the intensity of the lowest frequency mode (3116 cm^{-1}) increases significantly up to 0.3 GPa. Above this pressure, the relative intensities of this mode with respect to the other symmetric N−H stretching vibration start reducing. When the pressure reaches 10.9 GPa, this lowest frequency mode is too weak to be detected. In contrast to other modes, the obvious red shifts of the three peaks are observed with the application of pressure up to ∼14.6 GPa. The red shifts mean there are weak or moderate strength hydrogen bonds within oxamide, and the hydrogen bonds get stronger with increasing pressure.[38−40] Pressure can shorten the distance between H atoms and O atoms, accompanied by enhanced electrostatic attraction between them. This process can elongate N−H distance, causing the red shifts eventually. Apparently, the peak positions change

dx.doi.org/10.1021/jp302575k | J. Phys. Chem. B 2012, 116, 9796−9802

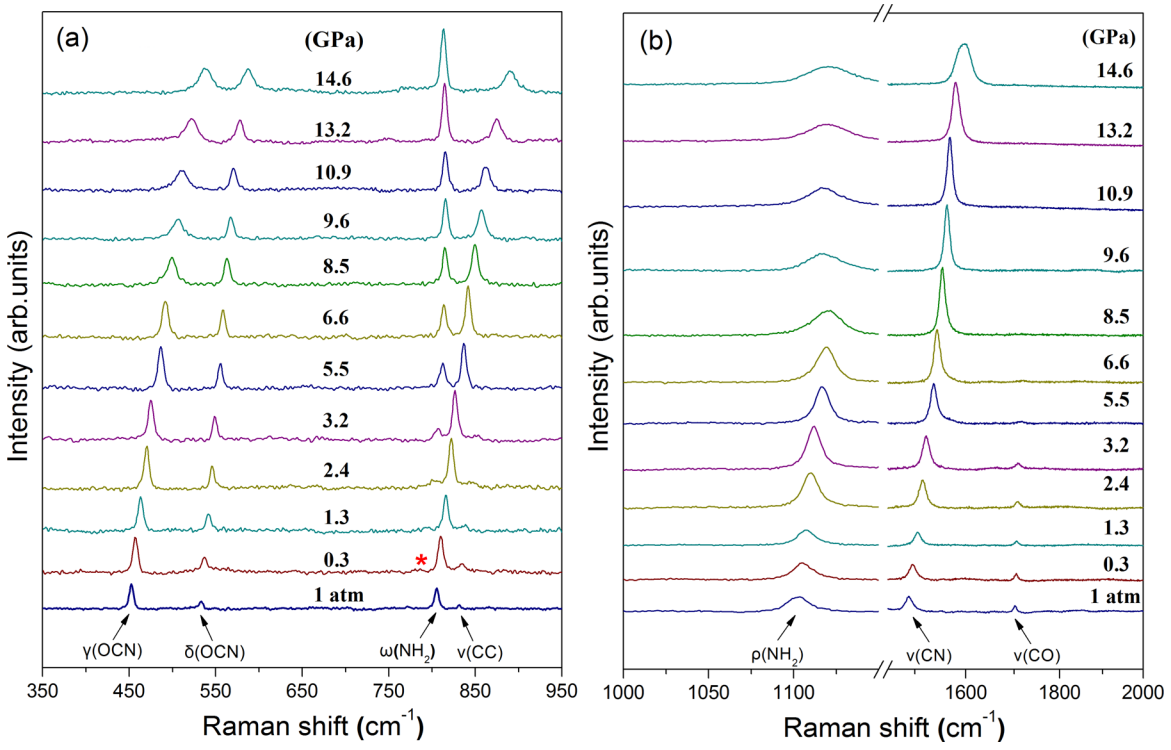

Figure 4. Raman spectra of oxamide as a function of increasing pressure in the wavenumber range 350−2000 cm^{-1}. The new peak is marked by an asterisk.

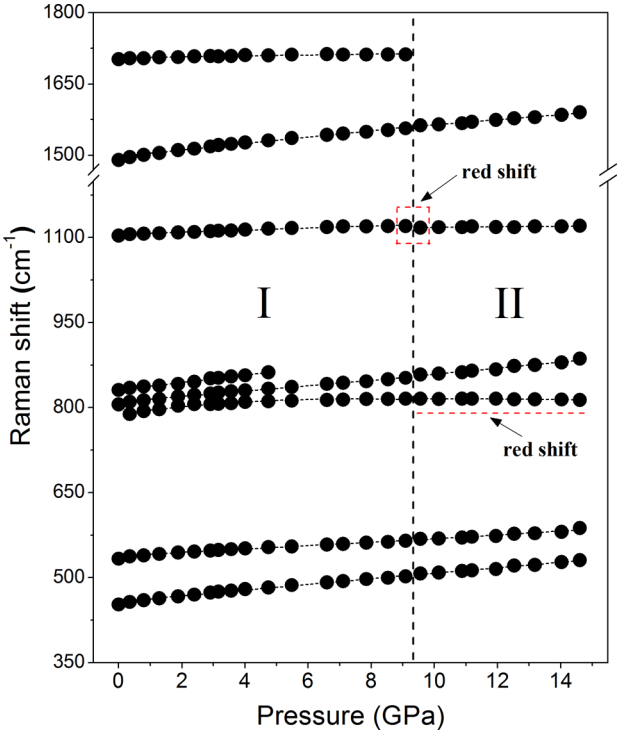

Figure 5. Frequency shifts of the corresponding Raman modes ranging from 350 to 2000 cm^{-1}. Linear fits are performed for clarity. The dotted line denotes the proposed phase boundary.

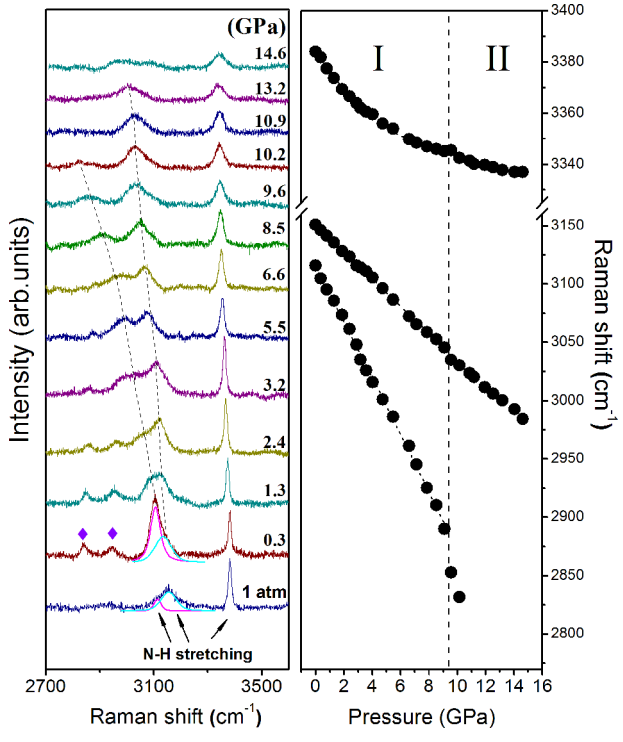

Figure 6. Raman spectra of oxamide at different pressures in the N−H stretching region 2700−3600 cm^{-1} (left); frequency shifts of these modes (right). The dotted line represents the boundary of the two phases, and the modes of methanol−ethanol−water mixture are marked by a rhombus.

dramatically at 9.6 GPa, revealing the proposed phase transition is correlated with the distortions of N−H···O bonded sheets.

In order to confirm the pressure-induced phase transition, we present the experimental data of ADXRD up to ∼17.5 GPa in Figure 7. The powder diffraction pattern of oxamide at ambient pressure is simulated using Material Studio software. Below 9.7 GPa, all the peaks shift to higher diffraction angles as the pressure is increased, indicative of a decrease of the interplanar

dx.doi.org/10.1021/jp302575k | J. Phys. Chem. B 2012, 116, 9796−9802

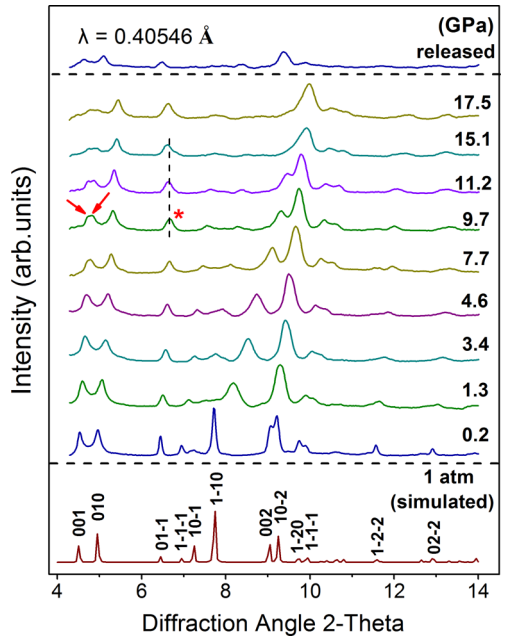

Figure 7. Selected ADXRD patterns of oxamide at different pressures. The wavelength for data collection is 0.40546 Å. The bottom pattern shows the simulated result under ambient conditions.

distance of crystal planes. At 9.7 GPa, the (001) peak is replaced by two peaks, of which the detailed decompositions under specified five pressures are shown in Figure 8. This

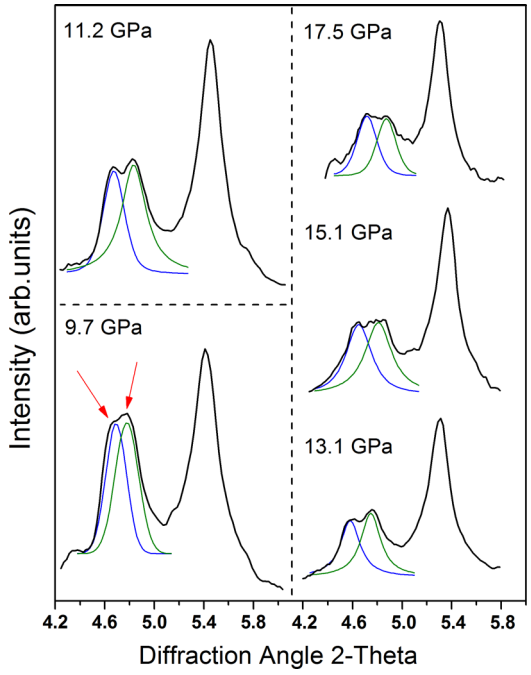

Figure 8. Decompositions of ADXRD patterns in the region 4.4−5.8° at specified five pressures.

change provides the most convincing evidence for the phase transition. Above 9.7 GPa, the peak marked by a star shifts to lower angle, which could be attributed to the increase of the (1−1−1) interplanar distance caused by the rotation of molecules. This transition pressure is consistent with that of the Raman measurement. With further compression, the new structure remains stable up to ∼17.5 GPa, the highest pressure in this study. The diffraction spectra of the two phases are similar, suggesting the two crystal structures are closely related. The diffraction pattern at 9.7 GPa returns to its initial state when the pressure is completely released.

The pressure dependences of the lattice parameters and unit cell volume are illustrated in Figure 9. As can be seen, the

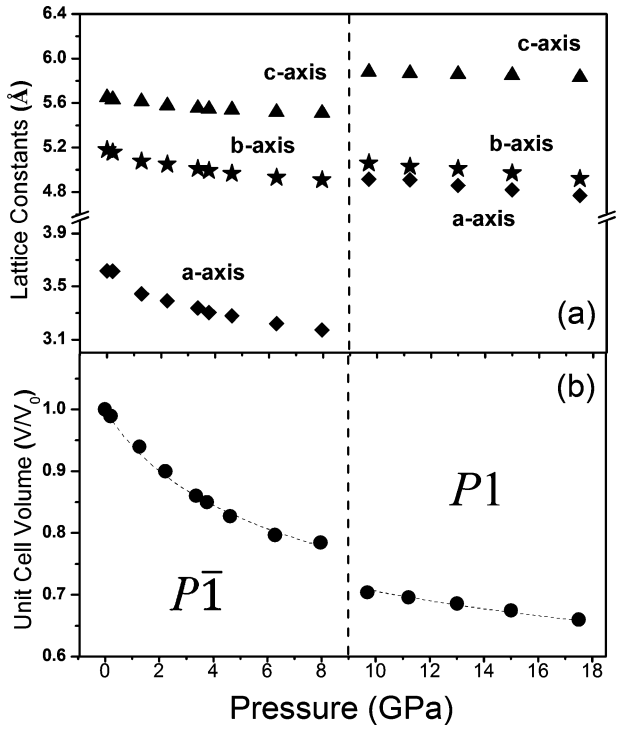

Figure 9. Compression of (a) lattice constants and (b) unit cell volume of oxamide with respect to pressure. The vertical dotted line represents the boundary of the two phases.

compression ratio of the *a*-axis is much higher than the *b*-axis and *c*-axis. This can be explained by the representative layered structure of oxamide. The molecules are connected by hydrogen bonds to form a layered structure in the *bc*-plane, whereas it is a much weaker van der Waals interaction along the *a*-axis. This accounts for the high compressibility of the *a*-axis. We conclude that oxamide has a high and anisotropic compressibility which is common in organic crystals.[41−43] Meanwhile, the cell volume reduces significantly at 9.7 GPa, indicating the crystal structure is more compact in phase II.

To understand what changes are happening with respect to the structure of oxamide under high pressure, we perform Rietveld refinement of the ADXRD pattern at 9.7 GPa (Figure 10). The result suggests that the most likely structure of phase II is of space group *P*1. And the indexed lattice parameters are a = 4.95(1) Å, b = 5.03(4) Å, c = 5.85(9) Å, β = 117.46(5) °, and Z = 2 with unit cell volume V = 122.10(3) Å^3. The unit cell of phase II is given in Figure 11. The two molecules separate from the *bc*-plane, twist, and are not parallel anymore. It can be seen that each molecule still has four H-donors and four H-acceptors, although the hydrogen-bonded networks are distorted dramatically. This is in accordance with the fact that there is no splitting in N−H stretching modes and the amide modes in Raman spectra with ascending pressure.

According to this hydrogen-bonded model, we propose the following mechanism for the pressure-induced phase transition.

dx.doi.org/10.1021/jp302575k | J. Phys. Chem. B 2012, 116, 9796−9802

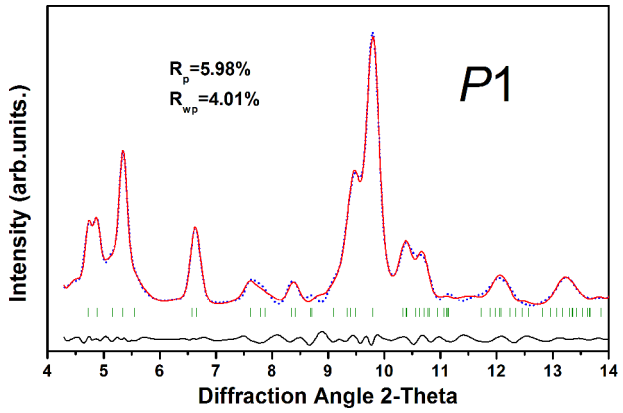

Figure 10. Rietveld refinement of the ADXRD pattern at ~9.7 GPa: red line, experiment; blue dotted line, simulated diffraction pattern for the *P*1 structure; the lower curve is the fit residual.

Hydrogen bonds and van der Waals forces are the dominant interactions within oxamide. It is the layered structure of oxamide crystal and the cooperation between the two forces that control the process of phase transition. With the increase of pressure, the interlayer distance in the crystal reduces apparently, leading to strengthened van der Waals interaction between them. Meanwhile, the hydrogen bonds within each layer also get enhanced with the reduction of distance between the molecules in the layers under the influence of high pressure. On further compression, the disturbed balance of the hydrogen bonds and van der Waals interactions brings about the expected instability to the layered structure. Moreover, the strengthened hydrogen bonds and van der Waals interactions make a contribution to an increase of free energy. With further compression to about 9.6 GPa, the hydrogen-bonded networks cannot support the increased Gibbs free energy. Then, the hydrogen bonds undergo the distorted changes to reduce the free energy, resulting in the phase transition ultimately.

The proposed mechanism can be well verified in terms of the variations in Raman spectra. The changes of hydrogen bonds can be reflected by the N−H stretching modes and the amide modes. The changes of these modes at 9.6 GPa indicate the strong distortions of hydrogen bonds. After being released to ambient pressure, the distortions are recovered completely. Moreover, in the course of our experiments, we do not observe any chemical transformation concluded by Bridgman in 1937.[9] These results strongly suggest that hydrogen bonds play a decisive role in the observed pressure-induced structural phase transition.

CONCLUSION

In summary, we have studied the pressure-induced phase transition of oxamide using in situ Raman scattering up to ~14.6 GPa and angle-dispersive X-ray diffraction measurements up to ~17.5 GPa. The observed discontinuity in Raman shifts indicates a phase transition around 9.6 GPa, and the X-ray diffraction experimental data confirm this reversible transition. Phase II with *P*1 symmetry is stable up to the highest pressure in this study. We propose the distortions of the hydrogen bonds are responsible for this phase transition, which can be demonstrated by the N−H stretching modes and the amide modes in Raman spectra very well. We hope this paper will contribute to the structural stability of hydrogen-bonded molecular crystals under high pressure.

ASSOCIATED CONTENT

Supporting Information

Selected Raman spectra of oxamide under different kinds of pressure conditions: one with methanol−ethanol−water as a pressure-transmitting medium (PTM), one with liquid argon as a PTM, and one without any PTM (Figure S1). Peak positions of the N−H bending mode and the NH_2 rocking mode (Table S1). This material is available free of charge via the Internet at http://pubs.acs.org.

AUTHOR INFORMATION

Corresponding Author

*E-mail: zoubo@jlu.edu.cn.

Author Contributions

§These authors contributed equally to this work.

Notes

The authors declare no competing financial interest.

ACKNOWLEDGMENTS

The authors are grateful to Dr. Ho-kwang Mao and Prof. Jing Liu for help on experiments. This work is supported by the NSFC (Nos. 21073071 and 51025206), the National Basic Research Program of China (No. 2011CB808200), Changjiang Scholar and Innovative Research Team in University (No. IRT1132), and Project 20121041 Supported by Graduate Innovation Fund of Jilin University. This work was performed

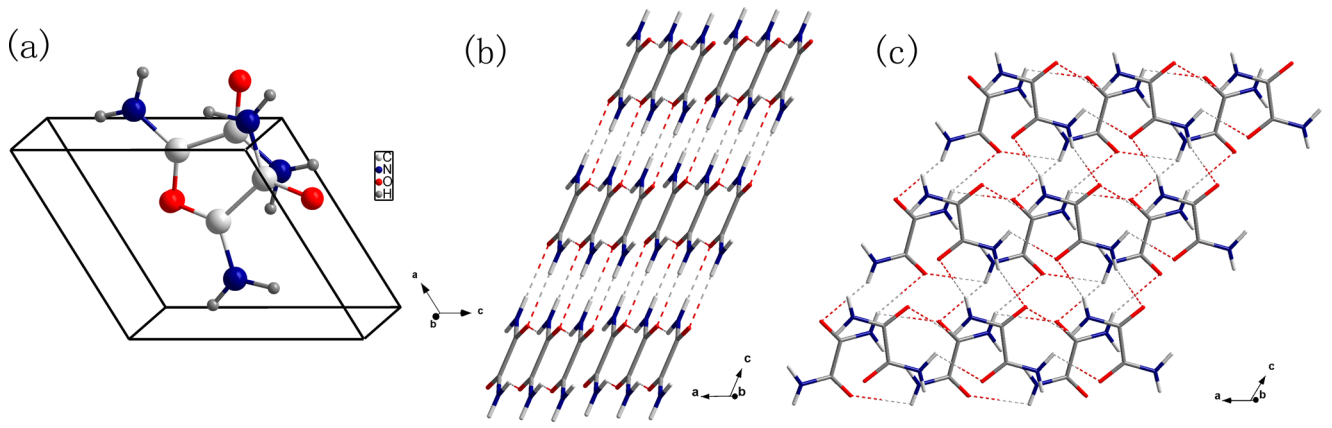

Figure 11. (a) The unit cell of oxamide at ~9.6 GPa; (b and c) the crystal structures of oxamide at ambient pressure and high pressure, respectively.

dx.doi.org/10.1021/jp302575k | *J. Phys. Chem. B* 2012, 116, 9796−9802

at HPCAT's beamline facility of the Advanced Photon Source at Argonne National Laboratory. HPCAT is supported by CIW, CDAC, UNLV, and LLNL through funding from DOE-NNSA, DOE-BES, and NSF. APS is supported by DOE-BES (No. DE-AC02-06CH11357). Portions of this work were performed at the 4W2 HP-Station, BSRF, which is supported by the Chinese Academy of Sciences (Grants KJCX2-SW-N20 and KJCX2-SW-N03). Portions of this work were performed at the BL15U1 at the SSRF.

REFERENCES

(1) Pickard, C. J.; Needs, R. J. *Nat. Mater.* **2008**, *7*, 775−779.
(2) Somayazulu, M.; Shu, J.; Zha, C.-s.; Goncharov, A. F.; Tschauner, O.; Mao, H.-k.; Hemley, R. J. *J. Chem. Phys.* **2008**, *128*, 064510.
(3) Olejniczak, A.; Ostrowska, K.; Katrusiak, A. *J. Phys. Chem. C* **2009**, *113*, 15761−15767.
(4) Shimizu, H.; Nagata, K.; Sasaki, S. *J. Chem. Phys.* **1988**, *89*, 2743−2747.
(5) Dziubek, K. F.; Katrusiak, A. *J. Phys. Chem. B* **2008**, *112*, 12001−12009.
(6) Johnstone, R. D. L.; Lennie, A. R.; Parker, S. F.; Parsons, S.; Pidcock, E.; Richardson, P. R.; Warren, J. E.; Wood, P. A. *CrystEngComm* **2010**, *12*, 1065−1078.
(7) Gajda, R.; Katrusiak, A. *Cryst. Growth Des.* **2011**, *11*, 4768−4774.
(8) Jeffrey, G. A.; Saenger, W. *Hydrogen Bonding in Biological Structures*; Springer-Verlag: Berlin, 1991.
(9) Bridgman, P. W. *Proc. Am. Acad. Arts Sci.* **1937**, *71*, 387−460.
(10) Bridgman, P. W. *Proc. Am. Acad. Arts Sci.* **1938**, *72*, 227−268.
(11) Ayerst, E. M.; Duke, J. R. C. *Acta Crystallogr.* **1954**, *7*, 588−590.
(12) With, G.; Harkema, S. *Acta Crystallogr. B* **1977**, *33*, 2367−2372.
(13) Lehr, J. R.; Brown, E. H. *Nature* **1964**, *203*, 1168−1169.
(14) Zou, B.; Dreger, K.; Mück-Lichtenfeld, C.; Grimme, S.; Schäfer, H. J.; Fuchs, H.; Chi, L. F. *Langmuir* **2005**, *21*, 1364−1370.
(15) Prins, L. J.; Reinhoudt, D. N.; Timmerman, P. *Angew. Chem., Int. Ed.* **2001**, *40*, 2382−2426.
(16) Steiner, T. *Angew. Chem., Int. Ed.* **2002**, *41*, 48−76.
(17) Dreger, K.; Zou, B.; Mu, Z. C.; Galla, H. J.; Chi, L. F.; Fuchs, H.; Schäfer, H. J. *Langmuir* **2006**, *22*, 1619−1625.
(18) Abe, Y.; Harata, K.; Fujiwara, M.; Ohbu, K. *Langmuir* **1996**, *12*, 636−640.
(19) Wang, K.; Duan, D. F.; Wang, R.; Liu, D.; Tang, L. Y.; Cui, T.; Liu, B. B.; Cui, Q. L.; Liu, J.; Zou, B.; et al. *J. Phys. Chem. B* **2009**, *113*, 14719−14724.
(20) Wang, K.; Duan, D. F.; Wang, R.; Lin, A. L.; Cui, Q. L.; Liu, B. B.; Cui, T.; Zou, B.; Zhang, X.; Hu, J. Z.; et al. *Langmuir* **2009**, *25*, 4787−4791.
(21) Wang, R.; Li, S. R.; Wang, K.; Duan, D. F.; Tang, L. Y.; Cui, T.; Liu, B. B.; Cui, Q. L.; Liu, J.; Zou, B.; et al. *J. Phys. Chem. B* **2010**, *114*, 6765−6769.
(22) Li, S. R.; Li, Q.; Zhou, J.; Wang, R.; Jiang, Z. M.; Wang, K.; Xu, D. P.; Liu, J.; Liu, B. B.; Zou, G. T.; et al. *J. Phys. Chem. B* **2012**, *116*, 3092−3098.
(23) Park, T.-R.; Dreger, Z. A.; Gupta, Y. M. *J. Phys. Chem. B* **2004**, *108*, 3174−3184.
(24) Allan, D. R.; Clark, S. J. *Phys. Rev. Lett.* **1999**, *82*, 3464−3467.
(25) Boldyreva, E. V. *J. Mol. Struct.* **2004**, *700*, 151−155.
(26) Joseph, J.; Jemmis, E. D. *J. Am. Chem. Soc.* **2007**, *129*, 4620−4632.
(27) Mishra, A. K.; Murli, C.; Sharma, S. M. *J. Phys. Chem. B* **2008**, *112*, 15867−15874.
(28) Li, S. R.; Li, Q.; Wang, K.; Tan, X.; Zhou, M.; Li, B.; Liu, B. B.; Zou, G. T.; Zou, B. *J. Phys. Chem. B* **2011**, *115*, 11816−11822.
(29) Li, S. R.; Wang, K.; Zhou, M.; Li, Q.; Liu, B. B.; Zou, G. T.; Zou, B. *J. Phys. Chem. B* **2011**, *115*, 8981−8988.
(30) Mao, H.-k.; Bell, P. M.; Shaner, J. W.; Steinberg, D. J. *J. Appl. Phys.* **1978**, *49*, 3276−3283.
(31) Rao, R.; Sakuntala, T.; Arora, A. K.; Deb, S. K. *J. Chem. Phys.* **2004**, *121*, 7320−7325.
(32) Hammersley, A. P.; Svensson, S. O.; Hanfland, M.; Fitch, A. N.; Hausermann, D. *High Pressure Res.* **1996**, *14*, 235−248.
(33) Bleckmann, P.; Thibud, M. *J. Raman Spectrosc.* **1982**, *12*, 105−108.
(34) Bleckmann, P.; Thibud, M. *J. Mol. Struct.* **1982**, *80*, 331−334.
(35) Scott, T. A., Jr.; Wagner, E. L. *J. Chem. Phys.* **1959**, *30*, 465−469.
(36) Rao, R.; Sakuntala, T.; Godwal, B. K. *Phys. Rev. B* **2002**, *65*, 054108.
(37) Ciezak, J. A.; Jenkins, T. A.; Liu, Z.; Hemley, R. J. *J. Phys. Chem. A* **2007**, *111*, 59−63.
(38) Hamann, S. D.; Linton, M. *Aust. J. Chem.* **1976**, *29*, 1825−1827.
(39) Moon, S. H.; Drickamer, H. G. *J. Chem. Phys.* **1974**, *61*, 48−54.
(40) Reynolds, J.; Sternstein, S. S. *J. Chem. Phys.* **1964**, *41*, 47−50.
(41) Boldyreva, E. V. *J. Mol. Struct.* **2003**, *647*, 159−179.
(42) Dreger, Z. A.; Gupta, Y. M.; Yoo, C. S.; Cynn, H. *J. Phys. Chem. B* **2005**, *109*, 22581−22587.
(43) Orgzall, I.; Emmerling, F.; Schulz, B.; Franco, O. *J. Phys.: Condens. Matter* **2008**, *20*, 295206.